

DOI: 10.1002/cbic.200400452

# Regions of Tau Implicated in the Paired Helical Fragment Core as Defined by NMR

Alain Sillen,<sup>[a]</sup> Arnaud Leroy,<sup>[a, b]</sup> Jean-Michel Wieruszeski,<sup>[a]</sup> Anne Loyens,<sup>[c]</sup> Jean-Claude Beauvillain,<sup>[c]</sup> Luc Buée,<sup>[c]</sup> Isabelle Landrieu,<sup>[a]</sup> and Guy Lippens<sup>\*[a]</sup>

*We have studied the mature Alzheimer-like fibers of tau by fluorescence and NMR spectroscopy. Assembly of the protein into paired helical filaments after incubation with heparin at 37°C was verified by electron microscopy and size-exclusion chromatography. NMR spectroscopy on these mature fibers revealed different regions of residual mobility for tau: the N-terminal domain was found to maintain solution-like dynamics and was followed by a large domain of decreasing mobility; finally the core region was distinguished by a solid-like character. Heteronuclear-NOE*

*data indicate that the decreasing mobility is due to both a slowing down of the rapid nanosecond movements and the introduction of slower movements that lead to exchange broadening. Fluorescence spectroscopy confirmed the presence of this rigid core, and some degree of protection from hydrogen exchange for those residues was observed. Hence, our data give a more precise picture of the dynamics of tau when it is integrated into mature filaments and should provide further understanding of the molecular processes that govern aggregation.*

## Introduction

Electron microscopy of the thick bundles of parallel filaments that are present within diseased neurons of patients suffering from Alzheimer's disease (AD) has led to their description as intracellular paired double helices.<sup>[1]</sup> Together with extracellular plaques composed mainly of aggregated  $\beta$ -amyloid peptide, these helices are currently considered as the molecular hallmarks of the disease.<sup>[2]</sup> Initial research into the biochemical nature of these paired helical filaments (PHFs) was hampered by the possibility that material adhering to the fibers rather than the PHF itself was being observed. Later, the observation of a core region and a fuzzy outer coat for the PHFs<sup>[3]</sup> concentrated research efforts on the protein component(s) that made up the inner-core region. The fuzzy coat can be stripped off by pronase proteolytic digestion while leaving the overall morphology of the fibers intact, as observed by electron microscopy. This coat region was initially found to carry all the epitopes recognized by two different antisera against the microtubule-associated protein, tau.<sup>[3]</sup> However, the monoclonal antibody mAb423 raised directly against the PHF core, decorated pronase-treated filaments much more strongly than the untreated ones, and its epitope was mapped to a central 9.5 kDa fragment of the tau protein.<sup>[4]</sup> Therefore, both chemical and immunological marking led to the conclusion that at least part of the microtubule-associated neuronal-tau protein was the main constituent of the fibers. A precise definition of the core region was, however, not possible, especially as antibodies are not necessarily available against all parts of the protein.

Further studies by mass spectroscopy showed that tau in the PHFs is generally found in its hyperphosphorylated form.<sup>[5]</sup> The discovery that a phosphorylation-independent interaction between recombinant tau and sulfated glycosaminoglycans, such as heparin, can lead to the *in vitro* formation of Alzheimer-like filaments under physiological conditions<sup>[6]</sup> opened up

further avenues for the structural study of these filaments. Still, no detailed picture has emerged for the ultrastructure of PHFs at the individual amino acid level. One of the underlying reasons for the lack of structural information for tau—be it in its soluble form, in its physiologically relevant microtubule-associated form, or in its pathologically aggregated state (“PHF-tau”)—is that the polypeptide does not quite behave as a regular folded protein. A variety of macroscopic techniques including circular dichroism, infrared spectroscopy, and small-angle X-ray scattering for the isolated protein have concluded that tau in solution is a random coil.<sup>[7,8]</sup> However, fiber X-ray<sup>[9,10]</sup> electron-diffraction studies<sup>[11]</sup> have concluded that the core of both native filaments isolated from brain tissue and *in vitro*-assembled filaments is formed by a cross- $\beta$  structure. The macroscopic alignment of the individual proteins within this core are still under discussion.<sup>[12]</sup> Although NMR spectroscopy might seem a suitable tool for structural studies, the shear length of this protein, unfavorable amino acid composition, and its macroscopically unfolded nature have led to the general acceptance in the community that its study is out of reach with present technology. However, we have recently shown that the *ab initio* acceptance of its random-coil nature, which

[a] Dr. A. Sillen, Dr. A. Leroy, Dr. J.-M. Wieruszeski, Dr. I. Landrieu, Dr. G. Lippens CNRS—Université de Lille 2 UMR 8525, Institut Pasteur de Lille B.P. 245, 59019 Lille Cedex (France)  
Fax: (+33) 3-20-87-12-33  
E-mail: Guy.Lippens@pasteur-lille.fr

[b] Dr. A. Leroy  
Laboratoire de Biochimie Appliquée  
Faculté de Pharmacie à Châtenay-Malabry (Paris XI), Tour D4 2<sup>ème</sup> étage  
5 rue Jean-Baptiste Clément, 92296 Châtenay-Malabry Cedex (France)

[c] A. Loyens, Dr. J.-C. Beauvillain, Dr. L. Buée  
INSERM U422, Institut de Médecine Prédictive et Recherche Thérapeutique  
Place de Verdun, 59045 Lille Cedex (France)

has led to carbon chemical shift values and the possibility of considering tau as a collection of independent small peptides, can provide a general strategy for its NMR assignment.<sup>[13,14]</sup> Very recently, a complete assignment for the three-repeat microtubule-binding domain of the shortest isoform completed our partial assignment.<sup>[15]</sup> For the 441 adult isoform (tau441), we have reached a level of residue-specific assignment that exceeds 40%. This gives us the possibility to probe both the presence of elements of residual structure in the soluble form of the protein and to monitor its interactions with its molecular partners. In the present paper, we apply solution NMR spectroscopy in order to further detail the overall structure of PHFs. We aim to obtain precise information on those parts of the protein that are implicated in the core or in the fuzzy coat of the fibers. In agreement with previous data, we find that the N terminus of tau is not integrated into the core of the fibers and the microtubule-binding repeats share an enhanced rigidity. These two regions are separated by a region characterized by complex dynamics. Previous immunocytochemistry results equally contrast with our findings for the C terminus: we find that full mobility is not recovered despite pronounced accessibility, as demonstrated by deuterium exchange.

## Results

### Fluorescence spectroscopy of the aggregation process

In order to follow the kinetics of PHF-tau formation, aggregation was initiated by the addition of heparin to a sample of tau441 (80  $\mu\text{M}$ ). This was then incubated at 37°C, and the increase in thioflavin S (ThS) fluorescence was monitored.<sup>[16]</sup> At this protein concentration, ThS fluorescence is less accurate for the quantification of filament formation.<sup>[16]</sup> However, we consistently used 80  $\mu\text{M}$  of tau because this concentration is necessary for the recording of high-quality NMR spectra with our cryogenic probe head at 600 MHz in a reasonable time (see below). ThS fluorescence increased monotonously and leveled off after 5 h, thereby setting the timescale for the aggregation process (Figure 1a). Light scattering showed a concomitant signal increase on a similar timescale (Figure 1a). Both techniques are the present standard methods for monitoring and quantifying tau aggregation. The resulting curves indicated that our protein-heparin sample indeed aggregated at 37°C over several hours and that the process was complete after 24 h. When monitored at 20°C, however, the same process was considerably slower, with less than 6% of the fluorescence signal after 24 h; this is in agreement with data reported in the literature.<sup>[16]</sup>

Low salt, high temperature, and intermolecular disulfide bridge formation have been reported to be crucial factors for tau aggregation.<sup>[17,18]</sup> Whereas the first two factors should not appreciably vary at the higher protein concentrations needed for the NMR assay, we repeated the aggregation experiments using the ThS fluorescence assay with 80  $\mu\text{M}$  tau as a function of dithiothreitol (DTT) concentration. Our results are in agreement with literature data that were obtained at lower protein concentrations. We observe a higher slope in fluorescence in-

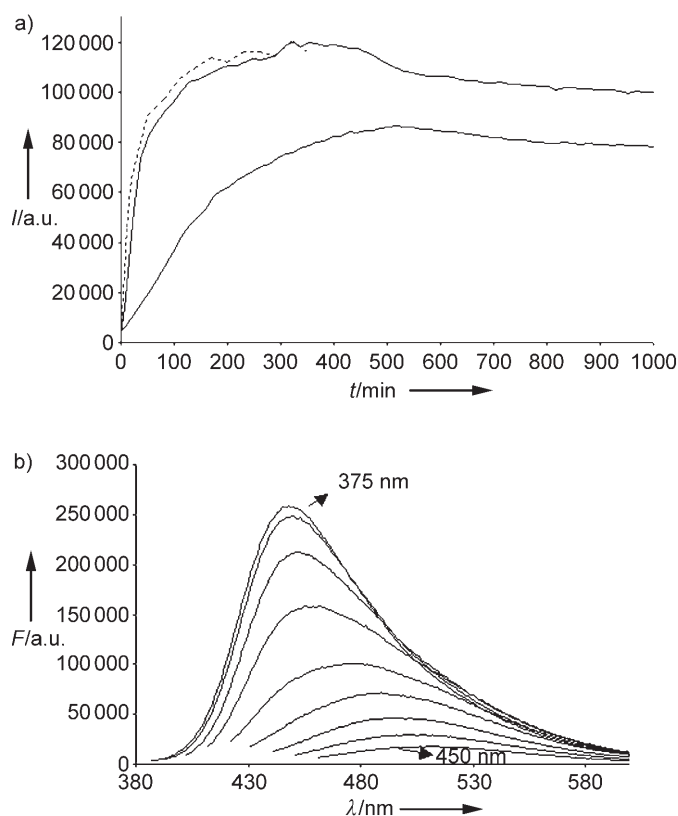


**Figure 1.** a) Time course for the aggregation of tau: heparin sample with DTT (300  $\mu\text{M}$ ) at 37°C as monitored by ThS fluorescence (upper solid curve) and light scattering (upper dotted curve). The lower curve corresponds to the ThS-fluorescence increase with 1 mM DTT. b) ThS fluorescence after its addition to a sample of tau that was incubated in the presence of heparin at 37°C for 5 h. The different curves correspond to the emission after excitation at varying wavelengths. Maximal intensity is found by excitation at 375 nm; the emission intensity gradually decreases when the excitation wavelength is varied from 380 to 450 nm.

crease when using 300  $\mu\text{M}$  rather than 1 mM of DTT (Figure 1a). This observation prompted our decision to use 300  $\mu\text{M}$  of DTT consistently for monitoring the aggregation behavior.

The emission spectrum is generally independent of the excitation wavelength because upon excitation into higher electronic and vibrational levels the energy quickly dissipates; this leaves the fluorophore in the lowest vibrational level of the lowest excited state.<sup>[19]</sup> However, when we monitored ThS fluorescence in a sample of PHF-tau after excitation at different wavelengths, we observed that the wavelength of maximal emission also shifted to longer wavelengths (Figure 1b). Such behavior for emission wavelength has been described for polar fluorophores that are embedded in a rigid environment where no redistribution of energies can occur; this results in a shift of the emission spectra to longer wavelengths when the excitation is on the red (long-wavelength) edge of the absorption spectrum.<sup>[20]</sup>

In conclusion, our fluorescence spectra set the timescale for the aggregation process under the conditions used. Furthermore, the observation of the red-edge effect indicates that the ThS assay monitors the appearance of a rigid core region in the growing fibers.

### Gel filtration and electron microscopy: macroscopic characterization of the fibers

Based on fluorescence and light-scattering assays, our sample reached steady state after 24 h. In order to verify that we had obtained bona fide PHFs, we investigated the morphology of the aggregates by electron microscopy (Figure 2). In the initial *in vitro* studies, in which heparin was used to assemble tau441 into Alzheimer like PHFs, straight rather than twisted fibers were obtained.<sup>[21]</sup> However, our filaments were mainly of the paired helical type. They had a typical length of 300–1000 nm, a width of 10–25 nm, and a cross-over repeat of roughly 80 nm (Figure 2). Thus, our NMR sample showed all characteristics of "Alzheimer PHFs".<sup>[1,22]</sup>

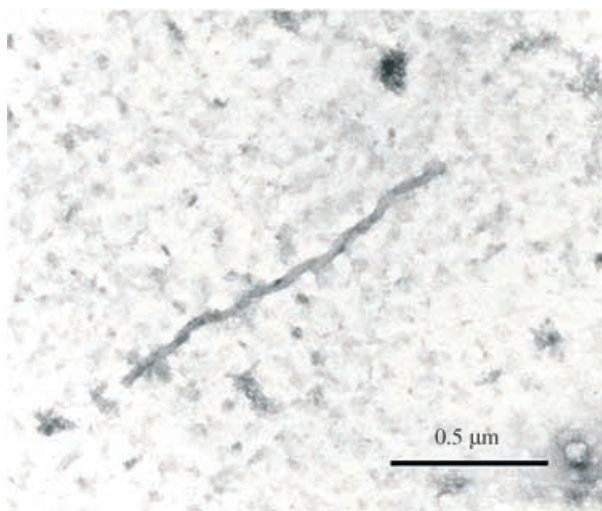


**Figure 2.** Electron microscope image of a representative PHF observed after incubation of tau with heparin for 24 h at 37 °C. The characteristic twisted pattern of a PHF can clearly be distinguished on the image.

Although at this stage we had confirmed the presence of PHFs in the NMR sample, we still needed to know the fraction of molecules in this fibrillar form. After 24 h of aggregation in the presence of heparin, a major fraction of the tau molecules was assembled into macroscopic structures, as witnessed by gel filtration data where the elution peak of the monomeric form had almost completely disappeared (Figure 3). Ultracentrifugation of the same sample confirmed that less than 10% of the initial material remained in solution (data not shown). Both experiments indicate that in the NMR studies discussed below, most if not all signal arises from tau that was integrated into fibers and not from free tau or tau integrated into low-oligomeric species.

### NMR spectroscopy: microscopic characterization of the fibers

The fibers are macroscopic and should therefore have a rotational tumbling time far beyond that of the GroEs/GroEl complex—the largest object so far studied by high-resolution

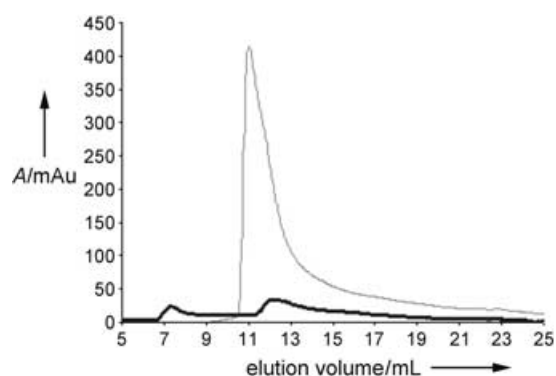


**Figure 3.** Elution profiles of tau free in solution (thin line) and of the same sample after assembly into fibers with heparin for 24 h (thick line).

NMR.<sup>[23]</sup> However, several examples have been reported where the residual mobility of a small subunit that is covalently linked to a large object is sufficient to obtain workable NMR spectra. One of the early examples of rotational freedom that was found to lead to high-quality NMR spectra was the observation of microtubulin-associated proteins in intact microtubules,<sup>[24]</sup> and more recently, the NMR study of the dynamics of one of the stalk domains in intact bacterial ribosomes.<sup>[25]</sup> The <sup>1</sup>H,<sup>15</sup>N correlation spectrum (HSQC) of the mature PHFs confirms this observation (Figure 4), as we indeed recover a significant fraction of the signals of the free protein. We started from the basic hypothesis that all peaks integrated in the rigid core of the PHF will behave as a true solid and therefore will be broadened beyond detection, whereas only peaks that correspond to residues that maintain their full mobility, although anchored to the macroscopic fibers, will not lose any intensity. Based on this assumption an accurate map of the different regions of PHF-tau becomes feasible. We can map our partial assignment for the full-length tau isoform onto those resonances that maintain their full intensity or that severely weaken in the PHF-tau spectrum.<sup>[13,14]</sup> Hence, we can distinguish different regions in the protein sequence according to their spectral appearance after assembly into PHFs. Comparison of the spectra of free and PHF-tau was furthermore possible in a quantitative way because chemical-shift differences for various residues between the two forms are very limited. Peak heights (which directly represent the  $t_2$  transverse relaxation time) were thus determined for all previously assigned and not overlapping correlation peaks in order to assess the intensity variation of the corresponding cross peaks upon integration of the tau molecule into the fibers.

At the N-terminal part of the protein, we recover full intensity for the amide peaks up to Ala77, with a mean value of  $1.02 \pm 0.04$  for the intensity ratio between free tau and PHF-tau cross peaks (Figure 5). The intensity then gradually drops and gives a value of 0.84 for Ala84 and a mean intensity ratio of  $0.79 \pm 0.03$  for the 50 amino-acid stretch that spans Thr101–Ala152, which resonates as the most downfield shifted isolated cross peak at (8.52 ppm, 129.3 ppm), as shown in Figure 4. The linear reduction of intensity continues with markers such as

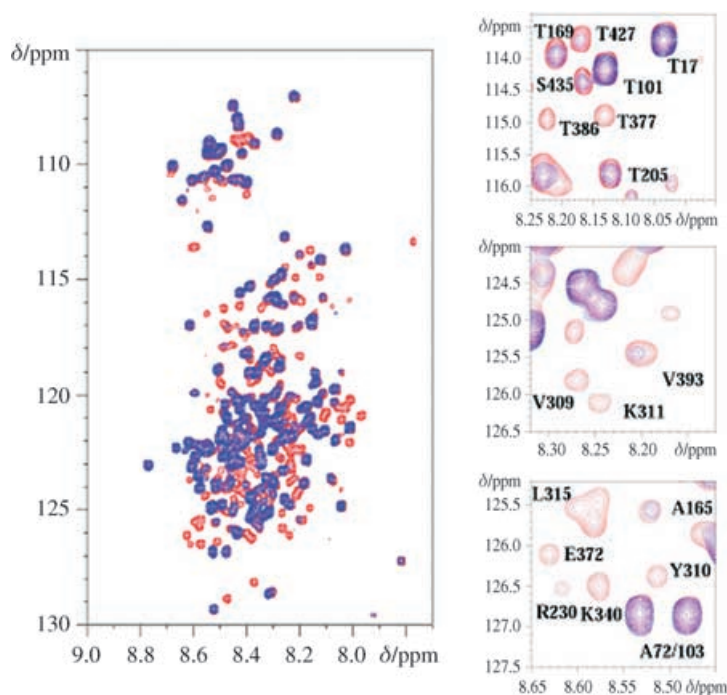


**Figure 4.** HSQC spectrum (full spectrum (top) and selected annotated zooms (bottom)) of tau free in solution (red) and integrated into mature PHFs (blue).

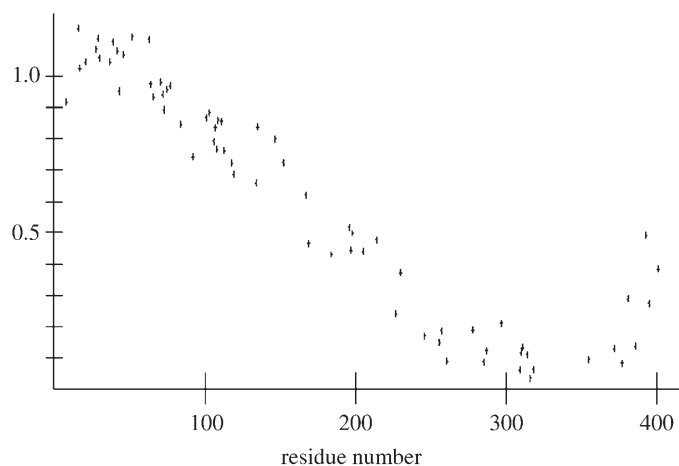


**Figure 5.** Ratio of the peak intensities in the spectra of free tau and PHF-tau. Only isolated peaks were taken into account.

Ala165, Thr169, and Thr205 (Figure 4), until it arrives at a region of tau where the intensity ratio is below 30%. This latter zone starts with the peaks from Ala227 (8.47 ppm, 128.8 ppm) and Arg230 (Figure 4), where both resonances still have some detectable intensity above the noise level in the mature PHF. The rigid PHF core, which we define as the region where the

intensity drops below 10%, starts with Gly261 and is further defined by 10 markers between Val309 and Thr386 that have a mean intensity ratio of  $0.09 \pm 0.01$ . This core region spans the fragment around Val309 and Lys311 (Figure 4) that was previously shown to be a nucleation site for the assembly of the fibers and can form fibers independently.<sup>[26,27]</sup> The last amino acid identified with a residual intensity lower than 10% is Thr377 which is situated just after the end of the fourth microtubule binding repeat. Past this zone and up to the C terminus of tau we find a symmetrical zone of reduced intensity with residues such as Val393 and Thr427 (Figure 4) characterized by a mean intensity ratio of  $0.36 \pm 0.05$ . For amino acids at the extreme C-terminal stretch of tau, the peak intensities that were observed in the soluble protein are not recovered. Indeed, even the last Leu441 residue that resonates as an isolated peak at (7.82 ppm, 127.4 ppm) recovers only 44% of its peak height in PHF-tau compared to the free protein (Figure 4).

A decrease in intensity can be provoked by an increased correlation time ( $\tau_c$ ), which describes the time-scale of the dipolar interaction between two nuclei that compose the reorienting amide vector. It can equally be defined by slow movements that lead to so-called exchange broadening.<sup>[28]</sup> Therefore, we performed a heteronuclear NOE experiment on free tau and the PHF sample. In this experiment, the intensity of the nitrogen magnetization is measured with or without proton saturation. This allows the extraction of a heteronuclear NOE effect for every amide group when performed in a 2D version.<sup>[29]</sup> In order to avoid problems of PHF sedimentation, the experiment on the PHF integrated tau was again performed on a 80  $\mu\text{m}$  sample. It therefore required over four days of measurement on a 600 MHz spectrometer with a cryogenic probe head. However, even then the peak intensities in the core region remained problematic. For the four isolated peaks at the most downfield nitrogen chemical shift, we could obtain NOE values even in the fibers because Ala246 retains 20% of its intensity compared to free tau (Figure 6). Intensity ratios between the proton saturated and reference spectra fluctuate for the different residues, but they remain negative for most residues in both free and PHF-tau forms. This indicates that rapid movements characterized by a  $\tau_c$  timescale below or around 1 ns

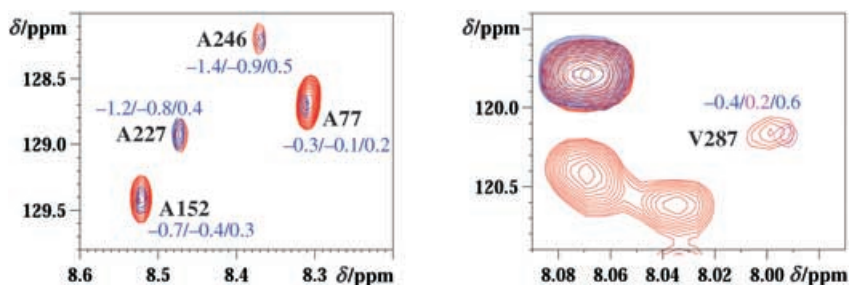


**Figure 6.** Heteronuclear-NOE spectra of PHF-tau without (red; positive contours) or with (blue; negative contours) proton irradiation. The numbers indicate the ratio between the peak intensities in the two spectra for tau/PHF-tau/difference between the latter values. The intensity ratio becomes positive for Val287 (with proton presaturation; blue = negative, magenta = positive contours).

dominate the heteronuclear NOE effect. For the residues that we defined in the core, peak intensity in the heteronuclear NOE spectra becomes very low, and only a few could be reliably integrated. Only for Val287 was the peak in the spectrum with proton saturation found to have the same sign as the reference spectrum starting from equilibrium nitrogen magnetization (Figure 6). Still, when we leave the N-terminal projection domain and approach the microtubule binding domain, the difference in NOE effect between free and PHF-tau increases from 0.2 for Ala77 to 0.6 for Ala246. Although the limited accuracy of the data in the region of strongly reduced mobility does not allow a precise quantitative analysis on a per-residue basis, the data generally indicate that rapid movements still dominate the NOE enhancement. The slowing down of these rapid movements is not sufficient to explain the apparent  $t_2$  decrease, since even doubling of the  $\tau_c$  value from 1 to 2 ns would only lead to a 30% increase of the  $t_2$  relaxation rate, according to the standard relaxation theory.<sup>[29]</sup> We thus conclude that the observed intensity decrease corresponds to a combined effect of increased local correlation times and additional slow motions for those fragments near the fiber core.

As a final NMR experiment, we performed a H/D exchange. For the free protein, exchange is very rapid over the whole polypeptide chain, since dissolving lyophilized tau into phosphate buffer with D<sub>2</sub>O leads to an empty spectrum in the amide-proton region (data not shown). Because lyophilization of the PHF-tau sample might alter the PHF structure and/or solubility, we performed the experiment by dissolving half of the PHF-tau sample in aqueous buffer in an equivalent volume of deuterated buffer. We recorded the HSQC spectrum immediately afterwards with 128 scans which led to a total measurement time of 5 h. Comparison of the reference and H/D exchanged spectra was performed by taking into account the dilution of the sample and the 50% replacement of protons with deuterium nuclei. Nonexchangeable peaks should thus have a similar intensity when compared with the initial spectrum that was recorded with only 64 scans; exchanged peaks should only have half the intensity. For residues in the N-terminal part we only recovered half of the intensity observed in the reference spectrum (Figure 7). This indicates that exchange is very rapid as is the case for all amide groups in free tau. However, for the central core region exchange was only partial and even absent for certain resonances, such as Tyr310. The behavior in the C-terminal tail of the protein that follows the microtubule binding repeats was less uniform; but our data indicate that exchange can happen to a large extent in this portion of the protein, despite the motional restriction deduced from the observed intensity drop.

## Discussion

The isolated neuronal tau protein is very soluble, and PHF formation in the absence of any cofactor probably requires the formation of cysteine-linked dimers.<sup>[17,18]</sup> The discovery that polyanions such as heparin,<sup>[6]</sup> RNA,<sup>[30]</sup> or arachidonic acid<sup>[31]</sup> promote the formation of Alzheimer-like PHFs has opened the way to further in vitro studies of the aggregation process and

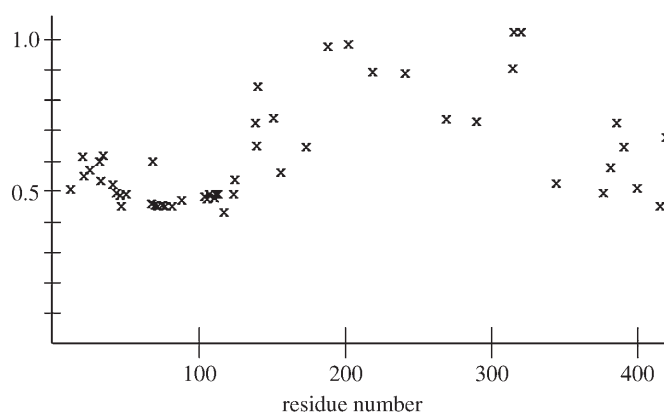


**Figure 7.** Intensity ratio of PHF-tau resonances in the H/D exchange experiment. A ratio of 0.5 indicates rapid full exchange, whereas a ratio of 1 corresponds to full protection.

of the final aggregated state. However, the physiological relevance of any of these cofactors in the diseased brain is at this moment not completely ascertained. Most recent studies have used macroscopic techniques that monitor the kinetics of aggregation into mature fibers. Light scattering and increased fluorescence after incorporation of ThS into the PHF core are commonly used, and electron microscopy is the technique of choice for the characterization of the morphology of the mature fibers.<sup>[32]</sup> However, as is the case for the isolated tau protein in solution, these techniques neither provide information on a per-residue basis of the aggregation process nor about the final mature paired helical fragment.

Although our NMR assignment is not yet completed, we show here that the obtained coverage allows the residual mobility of the polypeptide chain in the mature fiber to be mapped with a largely enhanced precision compared to protease cleavage and immunochemical methods.<sup>[3,4]</sup> Fibers obtained after incubation of tau with heparin for 24 h, display the characteristic paired helical feature as shown by electron microscopy (Figure 2). Moreover, their overall fiber form suggests a largely anisotropic rotational tumbling, but the shear size of the fibers with dimensions that exceed 10 nm even in the radial direction, should lead to a solid-like character for all spins that are tightly associated with the rigid core region. This is indeed what we observe, and the fact that a sizeable fraction of the peaks lose over 90% of their signal intensity correlates well with the absence of a sizeable amount of free tau, as observed by size exclusion chromatography (Figure 3). Both independent experiments indicate that most tau molecules are integrated into macroscopic PHFs after 24 h incubation with heparin.

After plotting the residual intensity of the different amides as a function of their location in the primary sequence (Figure 5), we obtain a schematic view of tau assembled into PHFs (Figure 8). The flexible N-terminal part of tau, defined here as the region in which the NMR peaks maintain their full intensity, covers part of the projection domain; Ala77 is again the last residue identified. This is in good agreement with the initially reported 17% of PHF mass that is lost after pronase

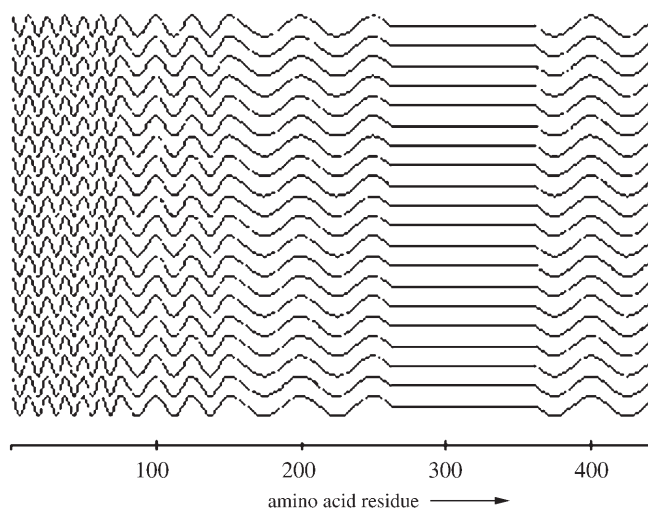


**Figure 8.** Schematic view of tau assembled into mature PHFs. The frequency of the sine wave indicates the residual mobility, where this term covers both rapid and slow motions (see main text). The first highly mobile zone extends from the N-terminal to Ala77. A second zone of linearly reduced mobility covers the primary sequence up to Gly261. The rigid core, defined by a residual intensity inferior to 10%, extends to Thr377. Finally, a second zone of reduced mobility covers the C-terminal part of tau.

treatment of PHFs isolated from the brain tissue of Alzheimer patients.<sup>[3]</sup> Furthermore, it shows that heparin-induced assembly not only gives good reproduction of the overall morphology of the fibers as seen with electron microscopy, but also other dynamical aspects of *in vivo*-formed PHFs.

Thioflavin dyes, which have been used to stain amyloid-like deposits and neurofibrillary tangles in postmortem brain tissue<sup>[33,34]</sup> were found early on to also interact with *in vitro*-formed tau fibers. They have allowed the development of a sensitive aggregation assay for the latter protein.<sup>[16]</sup> The fluorescence increase is generally interpreted in terms of increased cross- $\beta$  structure in the nascent fibers as aggregation gives rise to a dye-binding site. When we recorded fluorescence curves of ThS-bound PHF-tau during excitation at different wavelengths, the wavelength of maximal emission was found to shift upon variation of the excitation energy (Figure 1 b). This phenomenon was previously described as the "red-edge effect", and has been investigated in great detail by several groups who have related this phenomenon to the absence of dipolar relaxation of chromophore when it is embedded in a rigid environment.<sup>[20,35]</sup> Our experimental observation of the red-edge effect when ThS interacts with aggregated tau protein, therefore underscores the presence of a rigid environment in mature fibers (Figure 1 b).

Beyond this macroscopic detection of a region of enhanced rigidity, our NMR results allow precise mapping of the residues involved. The core region starts with Gly261, which is the first amino acid with a residual intensity below 10%. Gly261 has been successfully assigned as the only (Ile)Gly motif that differs between adult tau441 and the 352-amino-acid-long fetal isoform (tau352).<sup>[2]</sup> Furthermore, this residue is the reporter for Ser262, the phosphorylation of which prevents both microtubule binding and PHF formation.<sup>[36]</sup> The complete integration

of Ser262 in the immobile part of PHF and the protection of its amide function against H/D exchange (Figure 7) suggest that phosphorylation of this critical residue is an event that occurs before the protein is integrated into the fiber, thereby underscoring its regulatory role. In mature PHFs, the majority of the residues of the four tau441 repeats have lost most, if not all, of their intensity (except for the N-terminal half of the first repeat) and very little or no free tau remains in solution (Figure 3). We therefore conclude that the core region in the mature PHF equally spans the PHF<sub>6</sub> (<sup>306</sup>VQIVYJ<sup>311</sup>) or PHF<sub>6</sub>\* (<sup>275</sup>VQIINK<sup>280</sup>) peptides, which are considered to be nucleation sites for the fibrilization process and capable of independently forming filaments that incorporate ThS.<sup>[26,37]</sup>

The NMR assignment of Ala227 and Arg230 as isolated peaks (Figure 4) that lose a significant fraction of their intensity in the PHFs' spectrum (remaining intensities of 24 and 37%, respectively), together with Thr205, the intensity of which dropped by more than half, define a region of complex dynamics. Our measurement of line intensity rather than the peak integral effectively monitors line broadening and hence the motional aspects of the amide group. Significantly, when we integrated some of the truly isolated peaks (such as Leu441) with a spectral window of 60 Hz in both dimensions, we recovered the same value for the correlation peak in both spectra. This indicates that at least for this C terminus, the peak-intensity drop does not arise from either part of the molecules maintaining their full mobility or being distinguished by a solid-like character. For many other residues, however, the severe overlap of the spectra prevented a reliable integration for the verification of this statement; thus it might be that we only see a fraction of the polypeptides that maintain some flexibility, especially for the core region. Line broadening can be interpreted in terms of reduced mobility of the amide functions, but can be caused both by rapid and slow motions. The heteronuclear NOE data indicate that the rapid motions slow down in the vicinity of the rigid core, but not sufficiently to explain the observed broadening. An increase in slow dynamics at the level of its amplitude or the timescale involved, can therefore be deduced for this intermediate region.<sup>[28]</sup> This exchange broadening correlates well with the proximity, but not full integration of the amide groups, into the core region of the PHF. This resembles what we previously observed for peptide moieties that are anchored to the rigid polystyrene backbone used in solid-phase peptide chemistry.<sup>[38]</sup> When considering the intensity drop as a function of the primary sequence (Figure 5), we observe that a major part of the proline-rich region is contained in this zone of reduced mobility, which includes some of the major Ser/Thr motifs that are phosphorylated in both physiological and pathological conditions. Residues such as Thr231 and Ser235 are phosphorylation sites that are thought to be important for the aggregation process, and are recognized by the AT180 antibody after phosphorylation.<sup>[39]</sup> Upstream, we find the Ser237 and Ser238 doublet, which are defined as phosphorylated residues in PHFs isolated from AD neurons.<sup>[40]</sup> This *in vitro* study, in which heparin is used to assemble tau into PHFs, does not shed light on the integration of these residues in PHFs *in vivo*, but suggests that their phos-

phorylation after a phosphorylation-independent assembly might be problematic.

The rigid core does not quite extend to the extreme C terminus of tau, but stops at Thr377 and displays a linear increase in intensity for amino acids upstream of this residue. Interestingly, we do not recover the full intensity for the C-terminal residues, in contrast with the N-terminal stretch of full mobility, but we do observe significant hydrogen/deuterium exchange in this region. Therefore, it is not clear whether the C-terminal phosphorylation sites that include the AD2 epitope and the simultaneous phosphorylations at Ser396 and Ser404<sup>[41]</sup> will suffer from limited accessibility in the mature fiber. Equally, we cannot exclude that caspase cleavage at Asp421, which was recently shown to be of importance in AD tangle pathology,<sup>[42]</sup> will still happen after the assembly into fibers.

Our NMR results should be readily applicable to the assessment of tau assembly with other reagents, including arachidonic acid and/or RNA, thereby allowing further analysis of the common denominators that were proposed for these agents.<sup>[43]</sup> Other important questions concerning the fibrilization process should be equally addressable by NMR characterization of samples that have not fully assembled. These experiments, which are currently in progress at our laboratory, will shed light on the molecular basis of the aggregation of tau into Alzheimer's-like fibers.

## Experimental Section

**Sample preparation:** Expression and purification of tau441 were as previously described.<sup>[13,14]</sup> Recombinant tau (80  $\mu\text{M}$ ) was incubated with heparin (Sigma; average MW 16000) at a 1:10 molar ratio (heparin:tau) in an aqueous buffer containing sodium phosphate (25 mM), NaCl (25 mM), DTT (300  $\mu\text{M}$ ), pH 6.9, for 24 h at 37 °C. Assembly into fibers was monitored by using the ThS fluorescence assay.<sup>[16]</sup> ThS (Sigma, USA) concentration was maintained at 0.02 mg mL<sup>-1</sup> in all samples. Steady-state fluorescence was monitored on a PTI fluorescence spectrometer (PTI, Lawrenceville, NJ, USA). The excitation and emission slit widths were set to 2 and 4 nm, respectively, whereas polarizer was set to the magic angle. To monitor filament formation an excitation wavelength of 440 nm was used, whereas the emission spectrum was scanned from 450 to 600 nm.

To observe the red-edge effect of ThS, PHF were formed from tau (8  $\mu\text{M}$ ) and heparin (0.8  $\mu\text{M}$ ) and incubated for 6 h at 37 °C. Emission scans (380–600 nm) of ThS (0.02 mg mL<sup>-1</sup>) with different excitation wavelengths (375–450 nm) were taken after 24 h incubation at 20 °C.

**Size-exclusion chromatography:** After equilibration of a Superose-12 column (Amersham) with the same buffer as above (25 mM sodium phosphate, 25 mM NaCl, 300  $\mu\text{M}$  DTT, pH 6.9), tau (100  $\mu\text{L}$ ) in solution or an equivalent sample of tau:heparin obtained after 24 h of incubation at 37 °C, were injected with a small loop (50  $\mu\text{L}$ ) onto the column. Elution was performed at 0.5 mL/minute, and was monitored at 215 nm.

**Electron microscopy:** After incubation the original sample was diluted 100 times before a drop was placed on a formvar/carbon coated grid for 1 min. After drying, the grid was stained with 1% uranyl acetate for 2 min. Transmission electron microscopy was performed in a Zeiss model 901 electron microscope operated at 80 kV.

**NMR spectroscopy:** <sup>15</sup>N labeled samples of free or assembled tau (80  $\mu\text{M}$ ) were introduced in a 600 MHz spectrometer that was equipped with a cryogenic probehead (Bruker, Karlsruhe, Germany). Heteronuclear correlation <sup>1</sup>H–<sup>15</sup>N HSQC spectra were acquired with sensitivity-enhanced pulse sequences by using the WATERGATE sequence for water suppression.<sup>[44]</sup> NMR spectral parameters were recorded as previously described, with 64 scans per increment, and 256 complex points in the <sup>15</sup>N dimension.<sup>[13,14]</sup> Heteronuclear-NOE data were recorded with a standard-pulse sequence in an interleaved fashion with or without proton presaturation. The latter was obtained by a train of hard 120° pulses separated by 5 ms during the 5 s relaxation delay. The number of scans for this experiment was set to 192, which resulted in a total of 4 days for the experiment. Hydrogen/deuterium data were obtained by dissolving half of a PHF-tau sample into an equivalent volume of D<sub>2</sub>O buffer followed by immediate recording of the HSQC spectrum.

## Acknowledgements

We thank Dr. J. Dallongeville (Lille, France) and Dr. J. Christodoulou (Cambridge, UK) for careful reading of the manuscript. A.S. is funded by a European Training and Mobility Grant (HPRN-CT-2002-00241). The 600 MHz facility used in this study was funded by the Région Nord-Pas de Calais (France), the CNRS, and the Institut Pasteur de Lille. The electron microscope facility is supported by the IFR114 INSERM and the Imaging Core facility of the University of Lille 2. This work is supported by grants from CNRS, INSERM, and the European community (APOPIS project LSHM-CT-2003-503330).

**Keywords:** aggregation • electron microscopy • NMR spectroscopy • protein folding • protein structures

- [1] M. Kidd, *Nature* **1963**, 197, 192–193.
- [2] L. Buee, T. Bussiere, V. Buee-Scherrer, A. Delacourte, P. R. Hof, *Brain Res. Rev.* **2000**, 33, 95–130.
- [3] C. M. Wischik, M. Novak, P. C. Edwards, A. Klug, W. Tichelaar, R. A. Crowther, *Proc. Natl. Acad. Sci. USA* **1988**, 85, 4884–4888.
- [4] C. M. Wischik, M. Novak, H. C. Thogersen, P. C. Edwards, M. J. Runswick, R. Jakes, J. E. Walker, C. Milstein, M. Roth, A. Klug, *Proc. Natl. Acad. Sci. USA* **1988**, 85, 4506–4510.
- [5] M. Hasegawa, M. Morishima-Kawashim, K. Takio, M. Suzuk, K. Titani, Y. Ihara, *J. Biol. Chem.* **1992**, 267, 17 047–17 054.
- [6] M. Goedert, R. Jakes, M. G. Spillantini, M. Hasegawa, M. J. Smith, R. A. Crowther, *Nature* **1996**, 383, 550–553.
- [7] D. W. Cleveland, S. Y. Hwo, M. W. Kirschner, *J. Mol. Biol.* **1977**, 116, 227–247.
- [8] O. Schweers, E. Schonbrunn-Hanebeck, A. Marx, E. Mandelkow, *J. Biol. Chem.* **1994**, 269, 24 290–24 297.
- [9] G. G. Glenner, C. W. Wong, *Biochem. Biophys. Res. Commun.* **1984**, 120, 885–890.
- [10] D. A. Kirschner, C. Abraham, D. J. Selkoe, *Proc. Natl. Acad. Sci. USA* **1986**, 83, 503–5507.
- [11] J. Berriman, L. C. Serpell, K. A. Oberg, A. L. Fink, M. Goedert, R. A. Crowther, *Proc. Natl. Acad. Sci. USA* **2003**, 100, 9034–9038.
- [12] M. Margittai, R. Langen, *Proc. Natl. Acad. Sci. USA* **2004**, 101, 10 278–10 283.
- [13] G. Lippens, J. M. Wieruszkeski, A. Leroy, C. Smet, A. Sillen, L. Buee, I. Landrieu, *ChemBioChem* **2004**, 5, 73–78.
- [14] C. Smet, A. Leroy, A. Sillen, J. M. Wieruszkeski, I. Landrieu, G. Lippens, *ChemBioChem* **2004**, 5, 1639–1646.
- [15] D. Eliezer, P. Barre, M. Kobaslija, D. Chan, X. Li, L. Heend, *Biochemistry* **2005**, 44, 1026–11036.

- [16] P. Friedhoff, A. Schneider, E. M. Mandelkow, E. Mandelkow, *Biochemistry* **1998**, *37*, 10223–10230.
- [17] O. Schweers, E. M. Mandelkow, J. Biernat, E. Mandelkow, *Proc. Natl. Acad. Sci. USA* **1995**, *92*, 8463–8467.
- [18] K. Bhattacharya, K. B. Rank, D. B. Evans, S. K. Sharma, *Biochem. Biophys. Res. Commun.* **2001**, *285*, 20–26.
- [19] M. Kasha, *Discuss. Faraday Soc.* **1950**, *9*, 14–19.
- [20] A. P. Demchenko, *Luminescence* **2002**, *17*, 19–42.
- [21] M. Hasegawa, R. A. Crowther, R. Jakes, M. Goedert, *J. Biol. Chem.* **1997**, *272*, 33 118–33 124.
- [22] R. A. Crowther, *Proc. Natl. Acad. Sci. USA* **1991**, *88*, 2288–2292.
- [23] J. Fiaux, E. B. Bertelsen, A. L. Horwich, K. Wüthrich, *Nature* **2002**, *418*, 207–211.
- [24] R. W. Woody, D. C. Clark, G. C. K. Roberts, S. R. Martin, P. M. Bayley, *Biochemistry* **1983**, *22*, 2186–2192.
- [25] J. Christodoulou, G. Larsson, P. Fucini, S. R. Connell, T. A. Pertinhez, C. L. Hanson, C. Redfield, K. H. Nierhaus, C. V. Robinson, J. Schleucher, C. M. Dobson, *Proc. Natl. Acad. Sci. USA* **2004**, *101*, 10949–10954.
- [26] M. von Bergen, P. Friedhoff, J. Biernat, J. Heberle, E. M. Mandelkow, E. Mandelkow, *Proc. Natl. Acad. Sci. USA* **2000**, *97*, 5129–5134.
- [27] W. J. Goux, L. Kopplin, A. D. Nguyen, K. Leak, M. Rutkofsky, V. D. Shanmuganandam, D. Sharma, H. Inouye, D. A. Kirschner, *J. Biol. Chem.* **2004**, *279*, 26 868–26 875.
- [28] G. M. Clore, P. C. Driscoll, P. T. Wingfield, A. M. Gronenborn, *Biochemistry* **1990**, *29*, 7387–7401.
- [29] J. W. Peng, G. Wagner, *Biochemistry* **1992**, *31*, 8571–8586.
- [30] T. Kampers, P. Friedhoff, J. Biernat, E. M. Mandelkow, E. Mandelkow, *FEBS Lett.* **1996**, *399*, 344–349.
- [31] D. M. Wilson, L. I. Binder, *Am. J. Pathol.* **1997**, *150*, 2181–2195.
- [32] T. C. Gambelin, R. W. Berry, L. I. Binder, *Biochemistry* **2003**, *42*, 15 009–15 017.
- [33] P. S. Vassar, C. F. A. Culling, *Arch. Pathol.* **1959**, *68*, 487–498.
- [34] G. Kelényi, *J. Histochem. Cytochem.* **1967**, *15*, 172–180.
- [35] G. Weber, M. Shinitzky, *Proc. Natl. Acad. Sci. USA* **1970**, *65*, 823–830.
- [36] J. Biernat, N. Gustke, G. Drewes, E. M. Mandelkow, E. Mandelkow, *Neuron* **1993**, *11*, 153–163.
- [37] M. von Bergen, S. Barghorn, L. Li, A. Marx, J. Biernat, E. M. Mandelkow, E. Mandelkow, *J. Biol. Chem.* **2001**, *276*, 48 165–48 174.
- [38] G. Lippens, G. Chessari, J. M. Wieruszeski, *J. Magn. Reson.* **2002**, *156*, 242–248.
- [39] M. Goedert, R. Jakes, R. A. Crowther, P. Cohen, E. Vanmechelen, M. Vandermeeren, P. Cras, *Biochem. J.* **1994**, *301*, 871–877.
- [40] D. P. Hanger, J. C. Betts, T. L. Loviny, W. P. Blackstock, B. H. Anderton, *J. Neurochem.* **1998**, *71*, 2465–2476.
- [41] V. Buee-Scherrer, O. Condamines, C. Mourton-Gilles, R. Jakes, M. Goedert, B. Pau, A. Delacourte, *Mol. Brain Res.* **1996**, *39*, 79–88.
- [42] R. A. Rissman, W. W. Poon, M. Blurton-Jones, S. Oddo, R. Torp, M. P. Vitek, F. M. LaFerla, T. T. Rohn, C. W. Cotman, *J. Clin. Invest.* **2004**, *114*, 121–130.
- [43] S. Barghorn, E. Mandelkow, *Biochemistry* **2002**, *41*, 14 885–14 896.
- [44] M. Pioletto, V. Saudek, V. Sklenar, *J. Biomol. NMR* **1992**, *2*, 661–665.

Received: December 20, 2004

Revised: June 17, 2005